J|A|C|S
ARTICLES
Published on Web 03/27/2003

Mechanistic Studies of the Tellurium(II)/Tellurium(IV) Redox Cycle in Thiol Peroxidase-like Reactions of Diorganotellurides in Methanol

Youngjae You, Khalid Ahsan, and Michael R. Detty*

Contribution from the Department of Chemistry, University at Buffalo, The State University of New York, Buffalo, New York 14260-3000

Received December 6, 2002; E-mail: mdetty@acsu.buffalo.edu

Abstract: Di-*n*-hexyl telluride (**2**), di-*p*-methoxyphenyl telluride (**3**), and (*S*)-2-(1-*N*,*N*-dimethylaminoethyl)-phenyl phenyl telluride (**4**) catalyzed the oxidation of PhSH to PhSSPh with H_2O_2 in MeOH. Telluride **2** displayed greater rate acceleration than the diaryltellurides **3** and **4** as determined by the initial velocities, v_0, for the rate of appearance of PhSSPh determined at 305 nm by stopped-flow spectroscopy. Rate constants for the oxidation of tellurides **2**−**4** (k_{ox}), rate constants for the introduction of PhSH as a ligand to the Te(IV) center (k_{PhSH}) of oxidized tellurides **5**−**7**, and thiol-independent (k_1) and thiol-dependent (k_2) rate constants for reductive elimination at Te(IV) in oxidized tellurides **5**−**7** were determined using stopped-flow spectroscopy. Oxidation of the Te atom of the electron-rich dialkyl telluride **2** was more rapid than oxidation of diaryl tellurides **3** and **4**. The dimethylaminoethyl substituent of **4**, which acts as a chelating ligand to Te(IV), did not affect k_{ox}. Values of k_{PhSH} for the introduction of PhSH to oxidized dialkyl tellurane **5** and oxidized diaryl tellurane **6** were comparable in magnitude, while the chelating dimethylaminoethyl ligand of oxidized telluride **7** diminished k_{PhSH} by a fator of 10^3. Reductive elimination by both first-order, thiol-independent (k_1) and second-order, thiol-dependent (k_2) pathways was slower from dialkyl Te(IV) species derived from **2** than from diaryl Te(IV) species derived from **3**. The chelating dimethylaminoethyl ligand of Te(IV) species derived from **4** diminished k_1 by a factor of 50 and k_2 by a factor of 3 (relative to the **3**-derived species).

Introduction

Thiol peroxidases are excellent antioxidants and protect the body against the potentially damaging effects of lipid peroxidation and other oxidative damage.[1] Organoselenium and organotellurium compounds have shown thiol peroxidase activity and have therapeutic potential for a number of disease states.[2] The 1,2-benzoisoselenazol-3-one and analogues (potential antiinflammatories),[3] benzoselenazolinones,[4] selenamide derivatives,[5] diaryl diselenides,[6,7] glutaselenone (γ-glutamylselenocysteinylglycine),[8] selenosubtilisin,[9] and, more recently, seleninate esters[10] have all shown thiol peroxidase activity as have diorgano ditellurides.[11] While the catalytic cycle in these molecules encompasses several different mechanisms, most involve a selenenyl sulfide or tellurenyl sulfide intermediate.[5−7,10−13] Diorganotellurides have also shown thiol peroxidase-like activity,[14] but their mechanism of action has been little studied.[15] Herein, we describe the kinetics associated with each step of the catalytic cycle for the thiol peroxidase-like activity of several

(1) (a) Schwarz, K.; Foltz, C. M. *J. Am. Chem. Soc.* **1957**, *79*, 3292. (b) Flohe, L. In *Free Radicals in Biology*; Pryor, W. A., Ed.; Academic Press: New York, 1982; Vol. 5, pp 223−253. (c) *Selenium in Biology and Human Health*; Burk, R. F., Ed.; Springer-Verlag: New York, 1994.
(2) (a) Fong, M. C.; Schiesser, C. H. *Tetrahedron Lett.* **1995**, *36*, 7329. (b) Lin, F.; Geiger, P. G.; Giroti, A. W. *Cancer Res.* **1992**, *52*, 5282. (c) Siemann, D. W.; Beyers, K. L. *Br. J. Cancer* **1993**, *68*, 1071. (d) Lee, F. Y. F.; Allalunis-Turner, M. J.; Siemann, D. W. *Br. J. Cancer* **1987**, *56*, 33. (e) Bellomo, G.; Mirabelli, F.; DiMonte, D.; Richelmi, P.; Thor, H.; Orrenius, C.; Orrenius, S. *Biochem. Biopharmacol.* **1987**, *36*, 1313. (f) Tomashefsky, P.; Astor, M.; DeVere White, R. *J. Natl. Cancer Inst.* **1985**, *74*, 1233.
(3) (a) Sies, H. *Free Radical Biol. Med.* **1993**, *14*, 313. (b) Jacquemin, P. V.; Christiaens, L. E.; Renson, M. J.; Evers, M. J.; Dereu, N. *Tetrahedron Lett.* **1992**, *33*, 3863. (c) Chaudie're, J.; Moutet, M.; d'Alessio, P. C. R. *Soc. Biol.* **1995**, *189*, 861.
(4) Galet, V.; Bernier, J.-L.; Hénichart, J.-P.; Lesieur, D.; Abadie, C.; Rochette, L.; Lindenbaum, A.; Chalas, J.; Renaud de la Faverie, J.-F.; Pfeiffer, B.; Renard, P. *J. Med. Chem.* **1994**, *37*, 2903.
(5) (a) Reich, H. J.; Jasperse, C. P. *J. Am. Chem. Soc.* **1987**, *109*, 5549. (b) Back, T. G.; Dyck, B. P. *J. Am. Chem. Soc.* **1997**, *119*, 2079.
(6) Mugesh, G.; Panda, A.; Singh, H. B.; Punekar, N. S.; Butcher, R. J. *J. Am. Chem. Soc.* **2001**, *123*, 839.
(7) (a) Wilson, S. R.; Zucker, P. A.; Huang, R.-R., C.; Spector, A. *J. Am. Chem. Soc.* **1989**, *111*, 5936. (b) Iwaoka, M.; Tomoda, S. *J. Am. Chem. Soc.* **1994**, *116*, 2557. (c) Wirth, T. *Molecules* **1998**, *3*, 164. (d) Mugesh, G.; Panda, A.; Singh, H. B.; Punekar, N. S.; Butcher, R. J. *Chem. Commun.* **1998**, 2227.
(8) (a) Soda, K. *Phosphorus Sulfur Silicon* **1992**, *67*, 461. (b) Esaki, N.; Oikawa, T.; Tanaka, H.; Soda, K. *Biomed. Res. Trace Elem.* **1990**, *1*, 261.
(9) (a) Wu, Z.-P.; Hilvert, D. *J. Am. Chem. Soc.* **1990**, *112*, 5647. (b) House, K. L.; Dunlap, R. B.; Odom, J. D.; Wu, Z.-P.; Hilvert, D. *J. Am. Chem. Soc.* **1992**, *114*, 8573.
(10) Back, T. G.; Moussa, Z. *J. Am. Chem. Soc.* **2002**, *124*, 12104.
(11) (a) Engman, L.; Stern, D.; Cotgreave, I. A.; Andersson, C. M. *J. Am. Chem. Soc.* **1992**, *114*, 9737. (b) Kanda, T.; Engman, L.; Cotgreave, I. A.; Powis, G. *J. Org. Chem.* **1999**, *64*, 8161.
(12) Fischer, H.; Dereu, N. *Bull. Soc. Chim. Belg.* **1987**, *96*, 757.
(13) Haenen, G. R. M. M.; De Rooij, B. M.; Vermeulen, N. P. E.; Bast, A. *Mol. Pharmacol.* **1990**, *37*, 412.
(14) (a) Detty, M. R.; Gibson, S. L. *Organometallics* **1992**, *11*, 2147. (b) Engman, L.; Stern, D.; Pelcman, M.; Andersson, C. M. *J. Org. Chem.* **1994**, *59*, 1973. (c) Vessman, K.; Ekstörm, M.; Berglund, M.; Andersson, C. M.; Engman, L. *J. Org. Chem.* **1995**, *60*, 4461.
(15) Detty, M. R.; Friedman, A. E.; Oseroff, A. R. *J. Org. Chem.* **1994**, *59*, 8245.

10.1021/ja029590m CCC: $25.00

Scheme 1. Catalytic Cycle for Glutathione Peroxidase

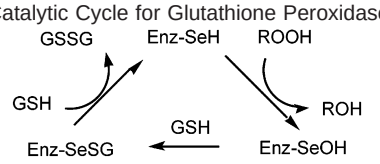

Scheme 2. Several Reactions of Selenenyl Sulfide and Tellurenyl Sulfide Intermediates

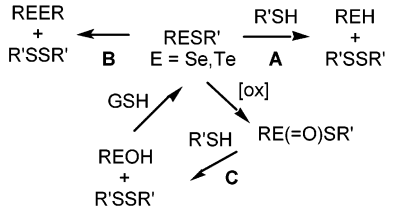

diorganotellurides using stopped-flow spectroscopy. These studies reveal two pathways for reductive elimination at Te(IV) and provide design parameters for more active diorganotelluride catalysts for not only thiol peroxidase-like reactions but also other H_2O_2-catalyzed processes.

As shown in Scheme 1, the selenium-containing enzyme glutathione peroxidase (Enz-SeH) is activated by a peroxy compound, which converts the selenol functionality to the corresponding selenenic acid and reduces the peroxy compound to the corresponding alcohol. The substrate glutathione (GSH) is next introduced to the activated enzyme forming the Enz-SeSG complex, which then reacts with a second molecule of GSH to regenerate the reduced enzyme and the oxidized disulfide product, GSSG.

One common feature of all of the proposed mechanisms of thiol peroxidase activity in Ebselen-like molecules, diselenides, ditellurides, selinic esters, or tellurininc esters above is the formation of a selenenyl sulfide or tellurenyl sulfide intermediate (analogous to the Enz-SeSG complex of Scheme 1) from a variety of precursors as shown in Scheme 2. Excess thiol can attack the selenenyl sulfide or tellurenyl sulfide intermediate directly to give disulfide and selenol or tellurol, which would reenter the catalytic cycle (path A).[5−7] In the original mechanism proposed for Ebselen and analogues, it was postulated that disproportionation of a selenenyl sulfide intermediate gave diselenide and disulfide[12] (path B), and later suggested that this process was catalyzed by thiol.[13] Oxidation of the diselenide would continue the catalytic cycle through the selenenic acid. Tellurenyl sulfides could undergo similar chemistry. Oxidation of selenenyl sulfide or tellurenyl sulfide intermediates to the corresponding seleninic or tellurinic thiol esters followed by attack of thiol to generate disulfide and the corresponding selenenic or tellurenic acid, which would reenter the catalytic cycle (path C), has also been proposed as a mechanistic path.[5b,10,11]

The proposed mechanism of glutathione peroxidase-like activity with diorganotellurides is summarized in Scheme 3.[14,15] Functionally, the steps are similar to those shown for glutathione peroxidase in Scheme 1. Oxidation of the telluride to the dihydroxy tellurane corresponds to activation of the enzyme, the introduction of GSH as a ligand corresponds to formation of the enzyme−substrate complex, and the reductive elimination step corresponds to regeneration of the reduced enzyme and the final oxidized, disulfide product. In these systems, the exchange of a sulfide ligand for a hydroxy ligand is followed by reductive elimination from the new diorgano Te(IV) intermediate with a sulfide ligand.

Scheme 3. Proposed Catalytic Cycle for Diorganotellurides in Thiol Peroxidase-like Reactions

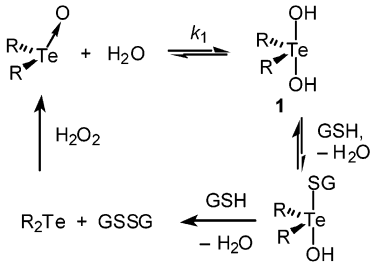

Unlike their lighter chalcogen analogues (sulfoxides and selenoxides), the telluroxides formed by the initial oxidation of a telluride with H_2O_2 are seldom isolated. In the presence of water, the telluroxide is converted to the dihydroxy tellurane **1**. The rate of addition of water, k_1, to the telluroxide as shown in Scheme 3 is on the order of 10^3 M^{-1} s^{-1} to form the dihydroxy tellurane, and equilibrium constants, K, for this process are on the order of 10−100 (with $[H_2O] = 55$ M).[16]

Following oxidation of the telluride, the thiol is introduced to the oxidized catalyst followed by reductive elimination of disulfide. Both of these steps have been observed by stopped-flow spectroscopy for the reaction of dihydroxy diphenyltellurane (**1**, R = Ph) with GSH in aqueous pH 7.4 buffer.[15] A fast initial reaction that followed overall second-order kinetics for equimolar concentrations of **1** (R = Ph) and GSH was followed by a second, slower reaction that followed pseudo first-order behavior in the presence of excess GSH. It was proposed that the initial fast reaction was the introduction of GSH into the coordination sphere of tellurium while the second slower reaction was the reductive elimination of GSSG from the Te(IV) intermediate to regenerate diphenyl telluride.[15] The exact mechanism of reductive elimination is unresolved.

Studies with GSH are limited by the solubility of the selenium- and tellurium-containing catalysts in an aqueous solvent. Comparison of catalytic activity among the various diselenides has been simplified through the method of Tomoda et al.[7b] in which thiophenol (PhSH) is a substitute for glutathione (GSH), H_2O_2 is used as the oxidant, and MeOH is used as solvent. In this procedure, catalytic activity is determined by the initial rates for the oxidation of PhSH (1.0×10^{-3} M) with H_2O_2 (3.75×10^{-3} M) in MeOH in the presence of a catalyst at a standard concentration of 1.0×10^{-5} M (eq 1). An obvious advantage of this procedure is the use of a solvent system more compatible with organochalcogenide and dichalcogenide catalysts that have minimal aqueous solubility.

$$H_2O_2 + 2\mathrm{PhSH} \xrightarrow[\mathrm{MeOH}]{\mathrm{catalyst}} 2H_2O + \mathrm{PhSSPh} \qquad (1)$$

In this paper, we follow the catalytic cycle of di-*n*-hexyl telluride (**2**),[17] di-*p*-methoxyphenyl telluride (**3**),[18] and (*S*)-2-(1-*N*,*N*-dimethylaminoethyl)phenyl phenyl telluride (**4**) with H_2O_2 and PhSH under the conditions of Tomoda et al.[7b] We have determined the catalytic activity for these tellurides as well as their rate constants for oxidation with H_2O_2. Using stopped-

(16) Engman, L.; Lind, J.; Merényi, G. *J. Phys. Chem.* **1994**, *98*, 3174.
(17) Butcher, T. S.; Detty, M. R. *J. Org. Chem.* **1999**, *64*, 5677.
(18) (a) Engman, L.; Persson, J.; Andersson, C. M.; Berglund, M. *J. Chem. Soc., Perkin Trans. 2* **1992**, 1309. (b) Engman, L.; Persson, J. *Organometallics* **1993**, *12*, 1068. (c) Serguievski, P.; Detty, M. R. *Organometallics* **1997**, *16*, 4386.

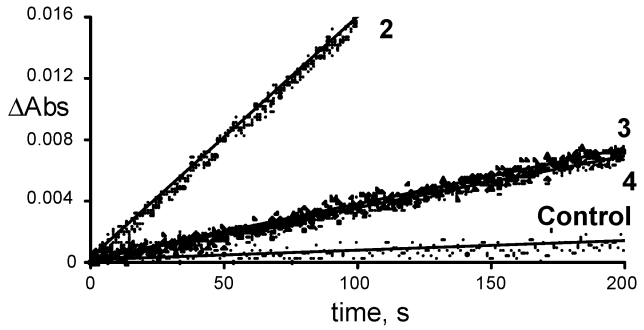

Figure 1. Initial rates of appearance of PhSSPh at 305 nm with 3.75×10^{-3} M H_2O_2, 1×10^{-3} M PhSH, and 1×10^{-5} M **2**−**4** in MeOH at 276.8 ± 0.4 K. The control reaction was run in the absence of catalyst.

Chart 1

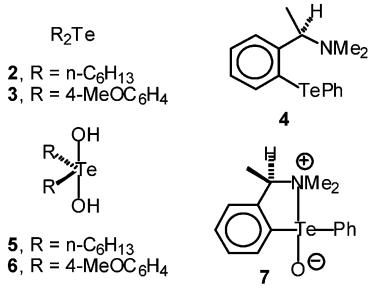

flow spectroscopy, we measured rate constants for the introduction of PhSH as a ligand and rate constants for the reductive elimination of PhSSPh from oxidized tellurides **5**−**7** (Chart 1). We note a change in mechanism for the rate-determining step of the reductive elimination from a thiol-independent path to a combination of thiol-independent and thiol-dependent pathways with increasing concentrations of PhSH and note that the rate-limiting step in the catalytic cycle is the rate of oxidation of the telluride.

Results and Discussion

Catalysis Studies. Tellurides **2**−**4** were examined as catalysts under the conditions of Tomoda et al.[7b] by mixing 5% CH_2Cl_2/MeOH solutions of catalyst (2.0×10^{-5} M) and PhSH (2.0×10^{-3} M) with equal volumes of a MeOH solution of H_2O_2 (7.5×10^{-3} M) in a stopped-flow spectrophotometer at 276.8 ± 0.4 K (final concentrations of 1.0×10^{-5} M **2**−**4**, 1.0×10^{-3} M PhSH, and 3.75×10^{-3} M H_2O_2). The rate of appearance of PhSSPh was monitored at 305 nm ($\epsilon = 1.24 \times 10^{-3}$ L mol^{-1} cm^{-1}).[7b] The 5% CH_2Cl_2 was added to keep the tellurides dissolved in the MeOH stock solutions. Linear increases in absorbance, k_0, were observed in the initial stages of the catalyzed reaction (Figure 1) and are listed in Table 1 in units of ΔA s^{-1}, where A is the absorbance at 305 nm. Values of k_0 were corrected for the uncatalyzed background reaction and were converted to initial velocities, v_0, in units of μM min^{-1}. All three catalysts **2**−**4** gave considerable enhancement in rate (v_0 of 35.6 μM min^{-1} for **2**, 8.5 μM min^{-1} for **3**, and 7.8 μM min^{-1} for **4**) relative to the uncatalyzed reaction (0.7 μM min^{-1}). To facilitate the tracking of rate constants, a graphical presentation of rate constants is provided in Figure 2.

As a control reaction for our slight modifications of the procedure of Tomoda et al.,[7b] we also examined PhSeSePh as a catalyst (Table 1, entry E). After correcting k_0 for the uncatalyzed background reaction, we found that v_0 for PhSeSePh

Table 1. Initial Rates of Oxidation (v_0) of PhSH (1×10^{-3} M) with H_2O_2 (3.75×10^{-3} M) in MeOH with Telluride Catalysts **2**−**4** (1×10^{-5} M), PhSeSePh (1×10^{-5} M), and Amine **14** (1×10^{-5} M) from Initial Linear Increases in Absorbance (k_0)[a]

entry	catalyst	k_0, ΔA s^{-1}[b]	v_0, μM min^{-1}
A	none	$(3.0 \pm 0.2) \times 10^{-6}$	0.72 ± 0.05
B	**2**	$(1.5 \pm 0.1) \times 10^{-4}$	35.6 ± 0.8
C	**3**	$(3.8 \pm 0.1) \times 10^{-5}$	8.5 ± 0.2
D	**4**	$(3.5 \pm 0.2) \times 10^{-5}$	7.8 ± 0.4
E	PhSeSePh	$(5.7 \pm 0.4) \times 10^{-6}$	0.65 ± 0.09 (0.55 ± 0.18)[c]
F	**14**	$(9.0 \pm 0.5) \times 10^{-6}$	1.4 ± 0.2

[a] Reagents were mixed in a stopped-flow spectrometer with a 2-mm path length at 276.8 ± 0.4 K, and initial rates were measured at 305 nm for the initial 5−10% of reaction. Values are the average of 7−10 independent runs with ± standard deviation. [b] Values of k_0 were corrected for the uncatalyzed reaction prior to calculation of v_0. [c] Reference 6.

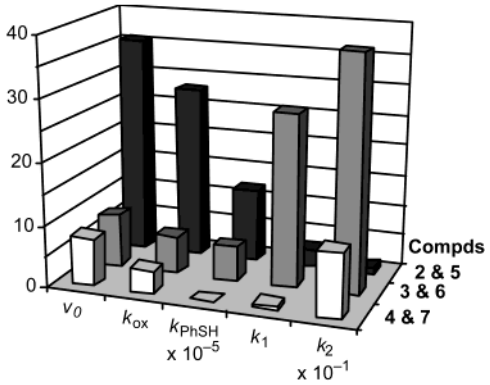

Figure 2. A graphical representation of relative values of the rate constants v_0, k_{ox}, k_{PhSH}, k_1, and k_2 discussed in this paper. Appropriate units and error limits are found in Tables 1 and 2.

in our assay is (0.65 ± 0.09) μM min^{-1}, which is in excellent agreement with the literature value of (0.55 ± 0.18) μM min^{-1}.[6] The uncatalyzed background reaction is somewhat larger using our conditions (0.72 ± 0.05 μM min^{-1}) relative to the reported value (0.15 ± 0.04 μM min^{-1}).[6] We measured identical uncatalyzed rates both in the stopped-flow spectrophotometer and in clean, 1-cm quartz cuvettes in a UV spectrophotometer using our conditions. The uncatalyzed reaction is sufficiently slow relative to the catalyzed reaction in our system such that the discrepancy has little impact on the results.

Tellurides **2**−**4** sample three different organotelluride structures: dialkyl tellurides, diaryltellurides, and organotellurides with a chelating ligand for higher oxidation states. *The chelating ligand of **4** minimizes the introduction of two ligands from solvent and PhSH.* All three classes demonstrate thiol peroxidase-like catalytic activity. We next examined the kinetics associated with oxidation, ligand exchange, and product formation via reductive elimination at tellurium.

Telluride Oxidation. The rates of oxidation of tellurides **2**−**4** with H_2O_2 were determined under pseudo first-order conditions in H_2O_2 (Table S1, Supporting Information). The electronic absorption spectra of tellurides **2**−**4** and their corresponding oxidized products **5**−**7**, respectively (Chart 1), are shown in Figures S1−S3 (Supporting Information). Loss of telluride was monitored at the long-wavelength absorption maximum of the telluride. The rate of oxidation of **2** in MeOH at a concentration of 5×10^{-4} M was followed at 276.8 ± 0.4 K using stopped-flow spectroscopy with H_2O_2 concentrations from 4×10^{-3} to 4×10^{-2} M (Table S1). A plot of k_{obs} versus [H_2O_2] was linear with a slope ($\pm 2\sigma$) of (2.80 ± 0.06) $\times 10^1$ L mol^{-1} s^{-1} (Table

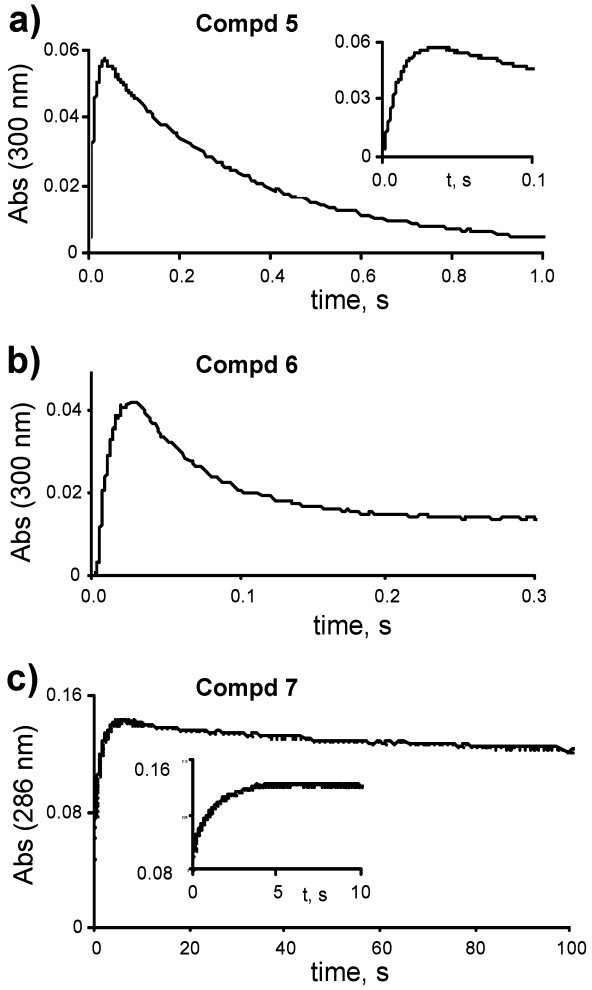

Figure 3. Kinetic traces for the reaction of (a) 4×10^{-5} M **5** and 4×10^{-5} M PhSH, (b) 4×10^{-5} M **6** and 4×10^{-5} M PhSH, and (c) 2×10^{-4} M **7** and 2×10^{-4} M PhSH in MeOH at 276.8 ± 0.4 K.

S1, Figure S4, Supporting Information). For the oxidation of telluride **3** at 276.8 ± 0.4 K, a plot of k_{obs} versus $[H_2O_2]$ was linear with a slope of 5.93 ± 0.04 L mol^{-1} s^{-1} (Table S1, Figure S5). For the oxidation of telluride **4**, a plot of k_{obs} versus $[H_2O_2]$ was linear with a slope of 3.61 ± 0.02 L mol^{-1} s^{-1} at 276.8 ± 0.4 K (Table S1, Figure S6). The various values of k_{ox} are compared in Figure 2.

Preparation of Oxidized Telluranes 5−7 for Stopped-Flow Studies. Compounds **2** and **3** were oxidized to the corresponding dihydroxy telluranes **5** and **6**, respectively, by treating the telluride with *N*-chlorosuccinimide (NCS) followed by hydrolysis of the intermediate chlorotelluronium intermediates with aqueous $NaHCO_3$.[19] Prepared in this manner, the dihydroxy telluranes were free of excess oxidant and could be used in MeOH solutions for kinetic studies without the introduction of H_2O_2. Similarly, telluride **4** was oxidized to **7** with NCS followed by hydrolysis with aqueous $NaHCO_3$. Methanol solutions of oxidized tellurides **2**−**4** (compounds **5**−**7**) were spectroscopically identical using either NCS or H_2O_2 as oxidant. The stoichiometric reaction of **5**−**7** with 2 equiv of PhSH in MeOH gave complete conversion to PhSSPh and tellurides **2**−**4**, respectively, as the only products. The reduced tellurides were isolated and were spectroscopically identical to starting tellurides **2**−**4**. Chiral telluride **4** showed no racemization.

(19) Detty, M. R. *J. Org. Chem.* **1980**, *45*, 274.

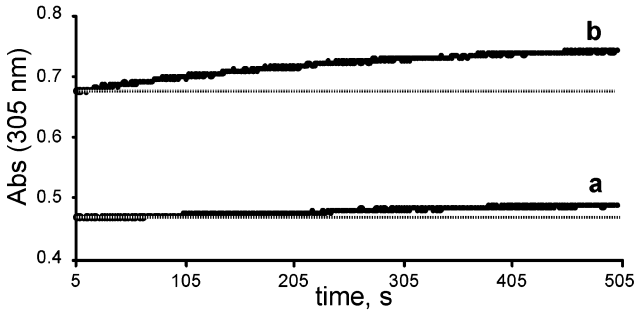

Figure 4. The third, slow reaction observed from 5 to 500 s with compound **6** at (a) 5×10^{-4} M **6** and 5×10^{-3} M PhSH and (b) 1×10^{-3} M **6** and 1×10^{-2} M PhSH in MeOH at 276.8 ± 0.4 K.

Scheme 4. Possible Equilibria of Dihydroxy Telluranes and Related Te(IV) Species in MeOH

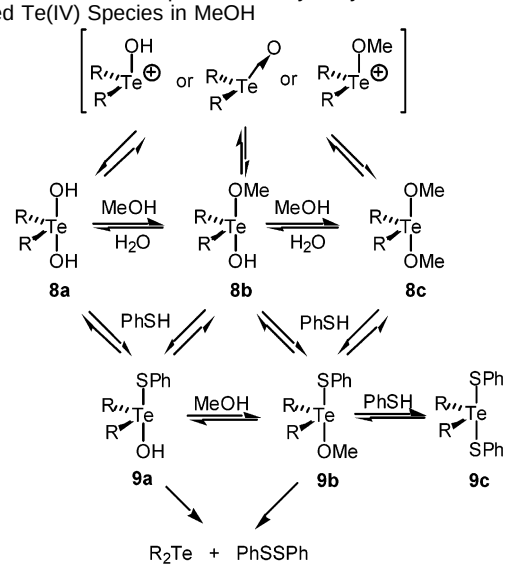

Stopped-Flow Studies. Solutions of **5** (8×10^{-5} M), **6** (8×10^{-5} M), and **7** (4×10^{-4} M) in 5% CH_2Cl_2−MeOH were mixed with equal volumes of solutions of PhSH (8×10^{-5} M for **5** and **6** and 4×10^{-4} M for **7**) in 5% CH_2Cl_2−MeOH in the stopped-flow spectrophotometer, and kinetic traces were observed at 300 nm for **5** and **6** and at 286 nm for **7**. Representative traces for these conditions are shown in Figure 3. For all three oxidized tellurides **5**−**7**, an initial fast reaction (reaction 1) was followed by a second slower reaction (reaction 2). We were unable to isolate reaction 1 from reaction 2 at different wavelengths. Values of k_{obs} were measured for both reaction 1 and reaction 2 over a range of concentrations of PhSH.

For compounds **5** and **6**, a third, slow reaction was observed that was monitored at 305 nm. This reaction was not observed with compound **7**. The rate of this reaction was dependent both on the concentration of **5** or **6** and on the concentration of PhSH. This reaction was more easily followed with compound **6**, and typical traces are shown in Figure 4.

As shown in Scheme 4, the reaction of an oxidized telluride with PhSH in MeOH is somewhat more complicated than that in water as a solvent. The telluroxide−dihydroxy tellurane equilibrium established in an aqueous environment can have additional products from MeOH addition, collectively represented as compounds **8** in Scheme 4. One would expect these intermediates also to incorporate PhSH as a ligand (giving

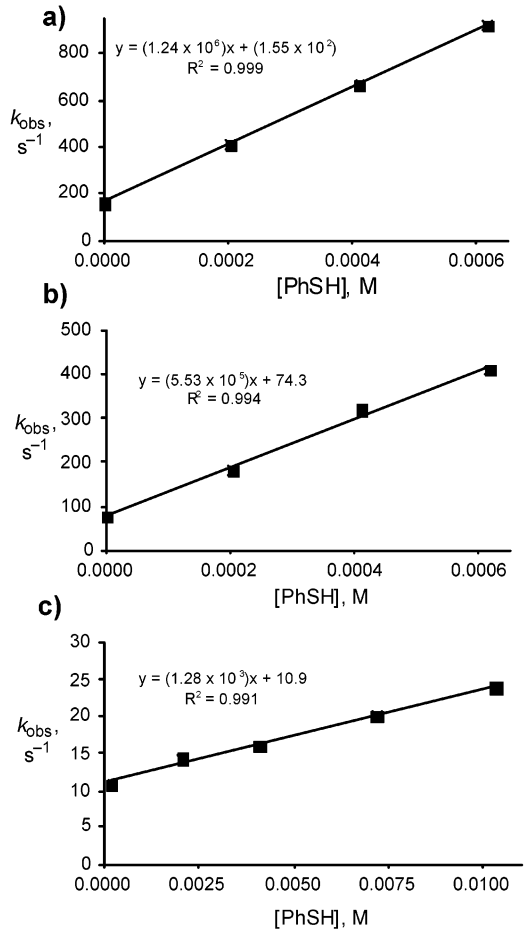

Figure 5. A plot of k_{obs} for the fast reaction (reaction 1) between PhSH and (a) compound **5** (4×10^{-5} M), (b) compound **6** (4×10^{-5} M), and (c) compound **7** (2×10^{-4} M) as a function of PhSH concentration under pseudo first-order conditions in MeOH at 276.8 ± 0.4 K. The slope of the line defines the second-order rate constant.

compounds **9**) and also to give PhSSPh through reductive elimination. We *assume* that equilibria involving solvent are established rapidly following oxidation of the telluride and that methoxy-containing species (especially **8b** and, perhaps, **8c**) will predominate in the equilibria among compounds **8**. Derivatives of **5**−**7** that incorporate one molecule of MeOH were identified by mass spectrometry using electrospray ionization of MeOH solutions of **5**−**7** (discussion in Supporting Information).

Reaction 1. The Introduction of PhSH. The rate of the initial fast reaction increased with increasing concentrations of PhSH (Table S2, Supporting Information), and pseudo first-order kinetics were followed as shown in Figure 5. The second-order rate constants, k_{PhSH}, were determined from the slope of the lines derived from a plot of k_{obs} versus [PhSH] to give values of k_{PhSH} ($\pm 2\sigma$) of $(1.20 \pm 0.01) \times 10^6$, $(5.5 \pm 0.2) \times 10^5$, and $(1.28 \pm 0.08) \times 10^3$ L mol^{-1} s^{-1} for **5**−**7**, respectively, at 276.8 ± 0.4 K. The values of k_{PhSH} are included in the graphical comparison of rate constants in Figure 2.

The introduction of PhSH to **5** and **6** proceeds with k_{PhSH}'s of 1.2×10^6 and 5.5×10^5 L mol^{-1} s^{-1}, respectively. These values are quite similar to the rate constants of 10^6−10^7 L mol^{-1} s^{-1} measured for the introduction of GSH to dihydroxy tellurane **1** (R = Ph) and related compounds.[16] When dissolved in MeOH, dihydroxy telluranes **5** and **6** would incorporate MeOH to give intermediate **8b** [and, perhaps, **8c** although no mass spectrometric evidence for species related to **8c** was observed (Supporting Information)], which can add PhSH to give intermediates **9** via the telluroxide or either a methoxytelluronium or hydroxytelluronium intermediate (Scheme 4).[16]

Scheme 5. Intramolecular N−Te(IV) Interactions

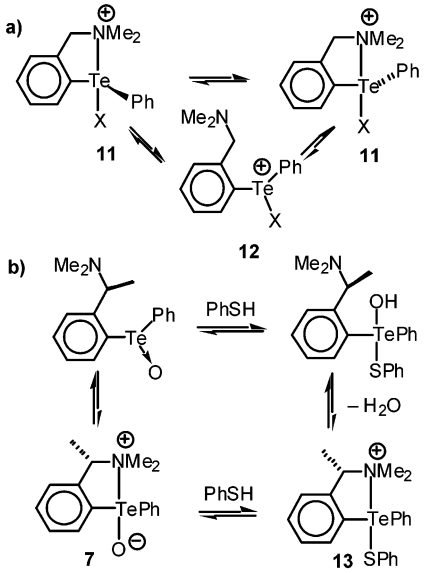

The initial reaction with PhSH is significantly slower for **7**, with a k_{PhSH} of 1.3×10^3 L mol^{-1} s^{-1}. This is most likely a consequence of the chelating 2-(1-*N*,*N*-dimethylaminoethyl)-phenyl ligand. X-ray studies of a structurally related system **11** (X = Br, Scheme 5a) have shown a partial Te−N bond of 2.389 Å from the interaction of the 2-(*N*,*N*-dimethylaminomethyl)-phenyl ligand and Te(IV).[20] Variable-temperature ^{1}H NMR studies with **11** (X = Br or I) indicate that the barrier to interconversion, $\Delta G^{\ddagger}$, of the two enantiomers of **11** is ~60 kJ mol^{-1} (with either halide) and involves breaking the Te−N bond to give either the bromotelluronium or the iodotelluronium intermediate **12**.[21] For compound **7**, addition of PhSH to the telluroxide (or a hydroxytelluronium intermediate) as shown in Scheme 5b must compete with intramolecular reattachment of the ligand, which would slow the rate of addition of PhSH.

Reaction 2. Reductive Elimination of PhSSPh. Formation of PhSSPh from the PhSH-containing complexes **9** involves reductive elimination at Te(IV). Several possible pathways are illustrated in Scheme 6. In one path, intermediates **9** can undergo direct nucleophilic attack by PhSH on the sulfide ligand to generate reduced telluride, PhSSPh, and MeOH, PhSH, or H_2O. In a second path, intermediates **9** can undergo solvolysis to generate thiotelluronium intermediates **10**, which then undergo nucleophilic attack by PhSH to give reduced telluride and PhSSPh. Alternatively, either intermediate could react with solvent to give PhSOMe and reduced telluride, with PhSOMe reacting further with PhSH to give PhSSPh. In all paths, the concentration of intermediate **9** would determine the velocity of the reaction leading to PhSSPh and reduced telluride. From the rate constants, k_{PhSH}, determined for reaction 1, incorporation of PhSH as a ligand to Te(IV) is rapid, but presumably reversible. The equilibrium constants between dihydroxy tel-

(20) Detty, M. R.; Friedman, A. E.; McMillan, M. *Organometallics* **1994**, *13*, 3338.
(21) Detty, M. R.; Williams, A. J.; Hewitt, J. M.; McMillan, M. *Organometallics* **1995**, *14*, 5258.

Scheme 6

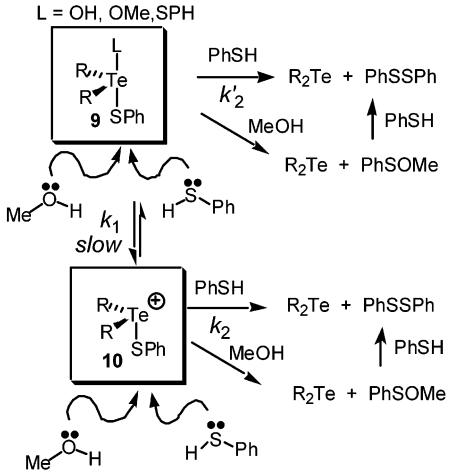

lurane and related intermediates **8** and thiol-containing intermediates **9** have not been determined.

In analogy to the glutathione peroxidase cycle of Scheme 1, reductive elimination from either **9** or **10** corresponds to the formation of product from the enzyme−substrate complex. In the reaction of di-*n*-hexyl dihydroxy tellurane (**5**) with PhSH, k_{obs} for reaction 2 (Figure 6a, Table S3) displayed saturation kinetics and reached a plateau where k_{obs} ($\pm 2\sigma$) remained constant at 29 ± 0.1 s^{-1} even with increasing concentrations of PhSH. Reaction 2 for di-*p*-methoxyphenyl telluride (**6**) was somewhat more complicated. Saturation kinetics were observed at concentrations of PhSH up to 1.6×10^{-3} M (inset, Figure 6b), where k_{obs} leveled off at 27.9 ± 0.2 s^{-1} between PhSH concentrations of 4×10^{-4} and 1.6×10^{-3} M. However, at concentrations of PhSH $\geq 1.6 \times 10^{-3}$ M, pseudo first-order kinetics were observed with a slope of $(3.81 \pm 0.06) \times 10^2$ L mol^{-1} s^{-1} for this region (Figure 6b).

Reaction 2 for compound **7** with the chelating 2-(1-*N*,*N*-dimethylaminoethyl)phenyl substituent did not show saturation kinetics as shown in Figure 6c. From an initial concentration of 2×10^{-4} M in PhSH, k_{obs} increased with the concentration of PhSH up to a concentration of PhSH of 2×10^{-3} M. At higher concentrations of PhSH, k_{obs} still increased but at a slower rate. Pseudo first-order kinetics were followed with a slope of $(1.03 \pm 0.02) \times 10^2$ L mol^{-1} s^{-1}.

In previous studies of the reaction of dihydroxy telluranes with thiols, reductive elimination at Te(IV) was observed to be first-order in both Te(IV) species and thiol.[15] It was suggested that nucleophilic attack of the thiol at the Te-coordinated sulfide gave disulfide and reduced telluride directly. The saturation kinetics observed in this study with **5** and **6** and increasing concentrations of PhSH suggest that another mechanistic path is also being followed.

The saturation kinetics observed for reaction 2 reveal two significant points about the reaction of **5** and **6** with PhSH: (1) The rapid increase in k_{obs} with increasing concentrations of PhSH is indicative that intermediates **8** and **9** in Scheme 4 are in equilibrium and that increasing concentrations of PhSH drive the equilibrium toward **9**. (2) The plateau regions for k_{obs} observed with both **5** and **6** are indicative that the concentration of intermediates **9** has reached a maximum, that is, the catalyst is saturated with substrate, and that the kinetics of reaction are no longer dependent on PhSH concentration. On the basis of this analysis, the rate-determining step in the reductive elimination at Te(IV) through the plateau regions is consistent either with direct displacement of PhSOMe from intermediates **9** with solvent or with a slow, first-order formation of thiotelluronium intermediates **10** followed by a fast reaction with either MeOH or PhSH (Scheme 6). Through the plateau region, a bimolecular reaction of intermediates **9** with PhSH does not appear to be a major contributor to the overall reaction (Scheme 7).

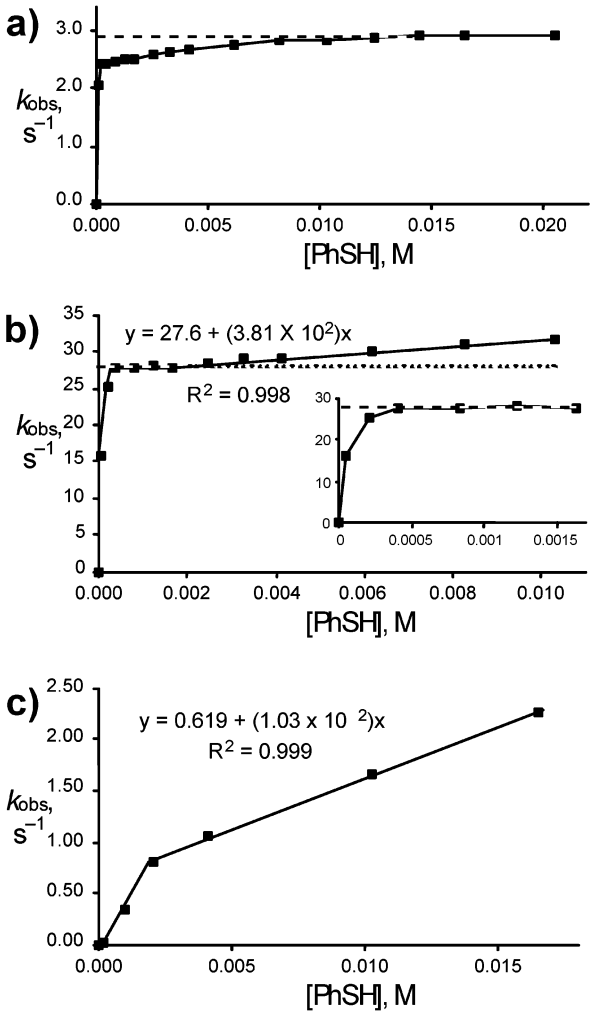

Figure 6. A plot of k_{obs} for the second reaction (reaction 2) between PhSH and (a) compound **5** (4×10^{-5} M), (b) compound **6** (4×10^{-5} M), and (c) compound **7** (2×10^{-4} M) as a function of PhSH concentration under pseudo first-order conditions in MeOH at 276.8 ± 0.4 K. For (b) and (c), the slope of the line defines the second-order rate constant.

For compound **6**, k_{obs} remained constant only between concentrations of PhSH of 4×10^{-4} and 1.6×10^{-3} M. At higher concentrations of PhSH, pseudo first-order kinetics were followed with a slope of 3.81×10^2 L mol^{-1} s^{-1}, which is consistent with a second mechanism for reductive elimination. Values of k_{obs} for compound **7** did not exhibit a plateau region. An inflection point for k_{obs} occurred at 2×10^{-3} M PhSH, followed by pseudo first-order kinetics with a slope of 1.03×10^2 L mol^{-1} s^{-1} for higher concentrations of PhSH. *The second-order rate constants, k_2, for reaction 2 of 3.8×10^2 L mol^{-1} s^{-1} for **6** and 1.0×10^2 L mol^{-1} s^{-1} for **7** are comparable in magnitude and suggest a similar process in the two systems.*

$$k_{obs} = k_1 + k_2[\mathrm{PhSH}] \qquad (2)$$

Table 2. Rate Constants for the Oxidation of Tellurides **2**−**4** with H_2O_2 (k_{ox}) and the Reactions of Oxidized Tellurides **5**−**7** with PhSH (k_{PhSH}, k_1, and k_2) in MeOH[a]

compound	k_{ox}, L mol^{-1} s^{-1}	k_{PhSH}, L mol^{-1} s^{-1}	k_1, s^{-1}	k_2, L mol^{-1} s^{-1}
2/**5**	28.0 ± 0.6	(1.20 ± 0.01) × 10^6	2.9 ± 0.1	<10
3/**6**	5.93 ± 0.04	(5.5 ± 0.2) × 10^5	27.9 ± 0.2	(3.81 ± 0.06) × 10^2
4/**7**	3.61 ± 0.02	(1.28 ± 0.08) × 10^3	0.62 ± 0.05	(1.03 ± 0.02) × 10^2

[a] Average (±2σ) of 7−10 independent runs at 276.8 ± 0.4 K.

Scheme 7

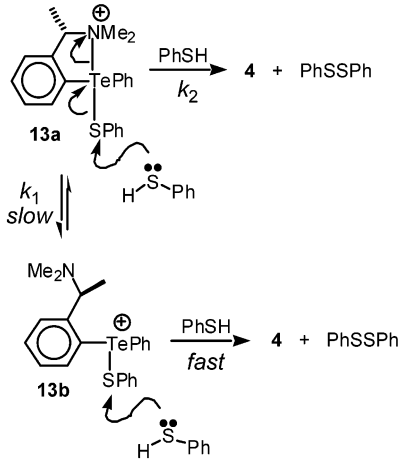

As shown in eq 2, k_{obs} for reaction 2 is composed of the rate constant for the first-order process, k_1, plus the product of the PhSH concentration and the rate constant for the second-order process, k_2[PhSH]. For compound **5**, the second-order process does not become competitive with the first-order process over the concentrations of PhSH that were examined. If one were to treat the slight rise observed between 5 × 10^{-3} and 1.5 × 10^{-2} M PhSH in Figure 6a as a pseudo first-order region, k_2 would be <10 L mol^{-1} s^{-1}. Consequently, k_{obs} and k_1 are essentially identical at saturation (2.9 s^{-1}). For compound **6**, both processes are discernible, and values of both k_1 and k_2 were determined (28 s^{-1} and 3.8 × 10^2 L mol^{-1} s^{-1}, respectively).

Compound **7** with a chelating 2-(1-*N*,*N*-dimethylaminoethyl)-phenyl ligand did not show the saturation kinetics associated with a predominate first-order reaction. However, the intercept of the pseudo first-order plot of Figure 6c suggests a value of k_1 (±2σ) of 0.62 ± 0.5 s^{-1} for the first-order process, which is significantly smaller than k_1 for either **5** or **6**.

The chelating ligand would be expected to slow solvolysis in the first-order process (intramolecular return of ligand from **13b** to regenerate **13a**) and would be a neutral leaving group in the second-order reductive elimination step as shown in Scheme 7. *The chelating ligand would also prevent the formation of intermediates related to* ***9c*** *in Scheme 4.* For compound **7**, the initial increase in k_{obs} with increasing concentrations of PhSH represents an increasing equilibrium concentration of intermediate **13**. However, the second-order process associated with compound **7** is competitive with the relatively slow first-order reaction at lower concentrations of PhSH than for either **5** or **6**. Consequently, no plateau region is observed, and only thiol-dependent kinetics are observed. Values of k_1 and k_2 for compounds **5**−**7** are compared graphically in Figure 2. A numerical summary of k_{ox}, k_{PhSH}, k_1, and k_2 for compounds **2**/**5**, **3**/**6**, and **4**/**7** is provided in Table 2.

Reaction 3. The "Slow" Reaction in MeOH. If solvent were involved directly in the reductive elimination step, then PhSOMe would be produced as the initial product and would then produce PhSSPh in a subsequent reaction with PhSH. To investigate this possibility, we prepared 0.08-M stock solutions of benzenesulfenyl chloride (PhSCl) in 1,2-dichloroethane[22] and diluted them to 1 × 10^{-3} M PhSCl in MeOH, to generate PhSOMe in situ. This solution was mixed with an equal volume of 2 × 10^{-2} M PhSH in MeOH in the stopped-flow spectrophotometer to give 5 × 10^{-4} M PhSOMe and 1 × 10^{-2} M PhSH. The rate of appearance of PhSSPh at 276.8 ± 0.4 K was monitored at 305 nm with a k_{obs} (±2σ) of (3.4 ± 0.1) × 10^{-3} s^{-1}. The rate of change in absorbance, k_0 (±2σ), during the initial part of the reaction was (7.1 ± 0.3) × 10^{-5} ΔA s^{-1}. These values are quite similar to those for the slow, third reaction for compound **6** as shown in Figure 4. For 5 × 10^{-4} M **6** and 1 × 10^{-2} M PhSH, k_{obs} was (1.6 ± 0.1) × 10^{-3} s^{-1}, and k_0 for the initial rate of change in absorbance was (4.7 ± 0.8) × 10^{-5} ΔA s^{-1}.

The similarity in rates suggests that PhSOMe is formed via a thiol-independent pathway in the reactions of compounds **5** and **6** and that the reaction of PhSOMe with PhSH to give PhSSPh as shown in Scheme 6 is the slow third reaction observed in the stopped-flow studies. This reaction was not observed with compound **7**, which has the smallest value of k_1. We note that the change in absorbance at 305 nm is small in this process, even with compounds **5** and **6**, and we cannot rule out the formation of some PhSOMe in the reaction of **7** with PhSH in MeOH. However, this process is less prevalent by at least an order of magnitude with compound **7** (k_1 = 0.62 s^{-1}) relative to compound **6** (k_1 = 28 s^{-1}).

Internal return of the chelating dimethylamino group of compound ***7*** *would reduce the products derived from the "free" thiotelluronium intermediate* ***13b*** *of Scheme 7 or products derived from an intermediate such as* ***9c*** *in Scheme 4.* The thiol-dependent reductive elimination would lead to more PhSSPh from direct reaction of PhSH with either **13a** or **13b** (Scheme 7) without the production of PhSOMe.

Telluride Oxidation as the Rate-Limiting Step in Thiol Peroxidase-like Activity. An understanding of the kinetics associated with the various steps of the catalytic cycle permits evaluation of the rate-limiting process in the catalytic cycle. Values of v_0 of 35.6 for **2**, 8.5 for **3**, and 7.8 μM min^{-1} for **4** for the rate of formation of PhSSPh with 1 × 10^{-5} M catalyst are quite similar to the initial velocities for oxidation of tellurides **2**−**4** to oxidized telluranes **5**−**7**, respectively. For telluride concentrations of 1 × 10^{-5} M, initial rates of oxidation of **2**−**4** with 3.75 × 10^{-3} M H_2O_2 are 69 for **2**, 13 for **3**, and 8.1 μM min^{-1} for **4** based on the second-order rate constants of Table 2.

For reaction 1, which is the introduction of PhSH, values of k_{PhSH} are 1.2 × 10^6 for **5** and 5.5 × 10^5 L mol^{-1} s^{-1} for **6**, which correspond to velocities of 7.2 × 10^5 and 3.3 × 10^5 μM min^{-1}, respectively, for formation of the catalyst−substrate

(22) Hamel, P. *J. Org. Chem.* **2002**, *67*, 2854.

Scheme 8

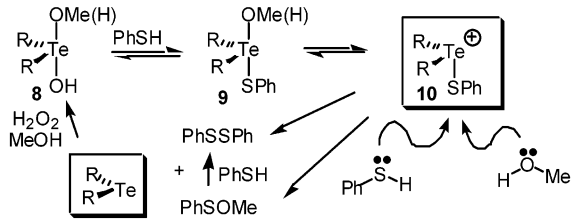

complex in the presence of 1×10^{-3} M PhSH and 1×10^{-5} M oxidized catalyst. While we do not know the equilibrium constant for the reaction of **5** or **6** with PhSH, it would lie toward products at 1×10^{-3} M PhSH on the basis of the "saturation" kinetics observed for the production of intermediates **9**.

The kinetics associated with reductive elimination in reaction 2 are also fast relative to the rate of oxidation. At 1×10^{-3} M PhSH, the rate of reductive elimination will be based on a concentration of essentially 1×10^{-5} M for the activated catalyst−substrate complex. With a k_{obs} of 2.5 s^{-1} at 1×10^{-3} M PhSH for reaction 2, the maximum rate of turnover of 1×10^{-5} M **5** is 1.5×10^{3} μM min^{-1} with respect to reductive elimination. For compound **6** with k_{obs} equal to 28 s^{-1} at 1×10^{-3} PhSH, the maximum rate of reductive elimination in the catalyst is 1.7×10^{4} μM min^{-1}. On the basis of the rate data for the introduction of PhSH to oxidized catalysts **5** and **6** and for the subsequent reductive elimination at Te(IV), the rate-limiting step in the catalytic cycle is the oxidation of the telluride with H_2O_2 for tellurides **2** and **3**.

The velocity for oxidation of 1×10^{-5} M **4** with 3.75×10^{-3} M H_2O_2 is 8.1 μM min^{-1}, which is nearly identical to a v_0 of 7.8 μM min^{-1} for the catalytic oxidation of PhSH with H_2O_2. Part of v_0 in the catalytic reaction is perhaps due to the amino substituent in the ligand, which can act as a general base to catalyze the oxidation of PhSH with H_2O_2. Amine catalysis has been shown in the thiol peroxidase-like reactions of amine-bearing diselenides.[6] We examined (*S*)-1-*N*,*N*-(dimethylamino)-1-phenylethane (**14**) as a model amine for telluride **4**. As shown in Table 1, **14** has a value of v_0 of 1.4 μM min^{-1} (Table 1, entry F), which suggests that the amino group in telluride **4** is contributing to the observed values of v_0.

Values of k_{PhSH}, k_1, and k_2 for tellurane **7** (Table 2) are significantly smaller than those for telluranes **5** and **6**. However, k_{PhSH} of 1.2×10^{3} L mol^{-1} s^{-1} for reaction 1 corresponds to a forward velocity of 7.2×10^{2} μM min^{-1} for the introduction of 1×10^{-3} M PhSH to 1×10^{-5} M **7**. The value of k_{obs} of 0.34 s^{-1} for reaction 2 with 1×10^{-3} M PhSH corresponds to roughly 50% of k_1 for saturation (0.62 s^{-1}) and a forward velocity of 1×10^{2} μM min^{-1} for reductive elimination of PhSSPh from 5×10^{-6} M intermediate **13** (Scheme 7). Even though the kinetics associated with the reaction of **7** with PhSH are slower than those for **5** and **6**, the maximum velocities associated with reaction 1 and 2 are still much greater than the velocity for oxidation of telluride, which remains as the rate-determining step in the catalytic cycle of **7**.

Summary and Conclusions

The basic mechanism of thiol peroxidase-like catalytic activity of **2**−**4** under the conditions of Tomoda et al.[7b] involves initial oxidation to the telluroxide/dihydroxy telluranes **5**−**7** followed by the cascade of reactions summarized in Scheme 8. Ligand exchange of PhSH involves reversible formation of telluroxide, hydroxy telluronium, and/or methoxy telluronium intermediates from intermediates **8** followed by addition of PhSH to give intermediates **9**. This process is reversible, and the equilibrium is driven toward intermediates **9** with increasing concentrations of PhSH. At higher concentrations of PhSH, intermediates such as **9c** in Scheme 4 cannot be rigorously excluded for reactions of **5** and **6**, although such intermediates are much less likely in compound **7** due to the chelating amine ligand. Intermediates **9** undergo reductive elimination to regenerate **2**−**4** and oxidized sulfur compounds via a thiol-independent pathway to generate PhSOMe via attack of MeOH on the sulfide ligand of **9** or via solvolysis of **9** to give thiotelluronium intermediates **10**, which then undergo attack by MeOH. The thiol-independent pathway can generate PhSSPh directly via a slow solvolysis reaction of **9** to give **10**, which then undergoes a rapid reaction with PhSH, which may not be competitive with MeOH at lower PhSH concentrations. At higher concentrations of PhSH, a thiol-dependent pathway emerges, which forms PhSSPh directly via nucleophilic attack of PhSH on the sulfide ligand of intermediates **9** or **10**.

For catalyst **4** with a chiral, chelating ligand, no racemization is observed in recovered catalyst. This observation suggests that all redox chemistry is occurring at the Te center and not at the amine (iminium intermediates are not involved) even though the amine is interacting with the oxidized Te center.

For the tellurides examined here, the rate-limiting step in the catalytic cycle is the oxidation of the telluride with H_2O_2. Typically, the rate of oxidation is greatest for more electron-rich diorganotellurides, which also correlates with the stability of the Te(IV) oxidation state. Dihexyl telluride **2** with two-electron donating alkyl groups is more readily oxidized to **5** than the two diaryltellurides **3** and **4** are oxidized to **6** and **7**, respectively. The introduction of PhSH as a ligand to the Te(IV) center is also more rapid with the electron-rich dihexyltellurane **5**. Because it is more electron rich, the Te(IV) center of **5** is more stable and does not undergo reductive elimination as readily as the Te(IV) center of **6** (Figure 2, values of k_1 and k_2 in Table 2). The chelating ligand of diaryltellurane **7** helps stabilize the Te(IV) center and helps to maintain trigonal-bipyramidal geometry at Te(IV).[20] Thus, both ligand exchange and reductive elimination are slower for **7** relative to **6** (Figure 2, values of k_1 and k_2 in Table 2).

For the diorganotellurides that have been examined as catalysts in thiol peroxidase-like reactions, the rate of introduction of thiol substrate and the rate of reductive elimination have had little impact on the turnover of catalyst. The rate of oxidation of Te(II) to Te(IV) is the rate-limiting step in the catalytic cycle. The catalytic rate and efficiency of diorganotellurides as thiol-peroxidase mimics can be increased further with the design of more readily oxidized catalysts.

Experimental Section

Preparation of Dihexyl Telluride (2) and Di-4-methoxyphenyl Telluride (3). Tellurides **2** and **3** were prepared according to refs 17 and 18, respectively.

For di-*n*-hexyl telluride (**2**): ^{1}H NMR (500 MHz, $CDCl_3$) δ 2.62 (t, 4H, J = 7.8 Hz), 1.73 (quintet, 4H, J = 7.5 Hz), 1.38−1.25 (m, 12H), 0.88 (t, 6H, J = 6.8 Hz); ^{13}C NMR (75 MHz, $CDCl_3$) δ 32.2, 31.7, 31.1, 22.5, 14.0, 2.6; λ_{max} (5% CH_2Cl_2−MeOH) 352 (ϵ = 380 M^{-1} cm^{-1}), 285 nm (ϵ = 960 M^{-1} cm^{-1}).

For di-*p*-methoxyphenyl telluride[18] (**3**): mp 47−49 °C; ^{1}H NMR (400 MHz, $CDCl_3$) δ 7.64 (AA′BB′, 4H, J ("doublet") = 7.2 Hz), 6.78

(AA′BB′, 4H, *J* ("doublet") = 7.2 Hz), 3.78 (s, 6H); ^{13}C NMR (75 MHz, $CDCl_3$) δ 160.2, 140.3, 115.9, 104.8, 55.7; λ_{max} (5% CH_2Cl_2−MeOH) 325(sh) nm (ϵ = 840 M^{-1} cm^{-1}).

Preparation of (*S*)-(2-[1-*N*,*N*-Dimethylamino)ethyl]phenyl)phenyl Telluride (4). To a solution of (*S*)-*N*,*N*-dimethylphenethylamine (0.89 g, 6.0 mmol) in dry pentane (20 mL) was added 1.7 M *t*-BuLi in pentane (3.8 mL, 6.6 mmol). After 3 h, phenyltellurenyl bromide (12 mL, 0.5 M in THF, 6.0 mmol) was slowly added, and stirring was continued for an additional 3 h. The reaction mixture was diluted with ethyl ether (25 mL), and the organic phase was washed with 1 N HCl (10 mL). The aqueous phase was extracted with ethyl ether (3 × 15 mL). The combined organic extracts were dried over $MgSO_4$ and concentrated. The crude product was purified by column chromatography on SiO_2 eluted with 5% ethyl ether in pentane to give 1.49 g (69%) of **4** as an off-white solid, mp 71−74 °C; $[\alpha]^{20}_D$ = −4.99 (*c* = 1.02, $CHCl_3$); IR (film, NaCl) 3057, 2978, 2935, 2855, 2823, 2780, 1577, 1428 cm^{-1}; ^{1}H NMR (400 MHz, $CDCl_3$) δ 7.90 (d×d, 2H, *J* = 1.0, 8.0 Hz), 7.35 (d×d×d, 1H, *J* = 2.0, 4.1, 8.0 Hz), 7.26 (d×d, 2H, *J* = 6.8, 8.0 Hz), 7.19 (d, 1H, *J* = 8.0 Hz), 7.15−7.10 (m, 2H), 6.90 (d×d, 1H, *J* = 2.0, 8.0 Hz), 3.63 (q, 1H, *J* = 7.2 Hz), 2.23 (s, 6H), 1.40 (d, 3H, *J* = 7.2 Hz); ^{13}C NMR (75 MHz, $CDCl_3$) δ 141.6, 140.3, 134.6, 129.0, 127.6, 127.3, 126.6, 125.7, 122.8, 122.3, 64.1, 39.6, 11.2; λ_{max} (5% CH_2Cl_2−MeOH) 286 nm (ϵ = 180 M^{-1} cm^{-1}); HRMS (ES) *m*/*z* 356.0612 (calcd. for $C_{16}H_{19}N^{130}Te + H^+$: 356.0658). Copies of ^{1}H and ^{13}C NMR spectra and the high-resolution electrospray mass spectrum are in the Supporting Information.

Preparation of Oxidized Tellurides 5−7.[19] Tellurides **2**−**4** (1 mmol) were dissolved in CH_2Cl_2 (2.5 mL) and MeOH (2.5 mL), and the resulting solution was cooled to 0 °C. *N*-Chlorosuccinimide (160 mg, 1.2 mmol) was added with stirring, and the resulting mixture was stirred for 5 min. Saturated aqueous $NaHCO_3$ (2.5 mL) was added, and the resulting mixture was stirred for 10 min at ambient temperature. The reaction mixture was poured into 20 mL of H_2O, and the products were extracted with CH_2Cl_2 (3 × 10 mL). The combined organic extracts were washed with saturated $NaHCO_3$ (10 mL) and brine, were dried over $MgSO_4$, and were concentrated to give **5**−**7** as waxy, colorless oils. These materials were prepared immediately before use and were used without further purification.

For **5** (95% yield): ^{1}H NMR (400 MHz, $CDCl_3$) δ 2.78 (br d×t, 4H, *J* = 4, 8 Hz), 1.90 (br s, 4H), 1.44 (br s, 4H), 1.32 (br s, 8H), 0.91 (br t, 6H, *J* = 7 Hz); λ_{max} (5% MeOH−CH_2Cl_2) 275 (sh) (ϵ = 1020 cm^{-1} M^{-1}), 237 nm (ϵ = 12 000 cm^{-1} M^{-1}); HRMS (EI) *m*/*z* 317.1122 (calcd for $[C_{12}H_{26}{}^{130}TeOH]^+$: 317.1124).

For **6** (92% yield): ^{1}H NMR (400 MHz, $CDCl_3$) δ 7.77 (br s, 4H), 6.85 (br s, 4H), 3.79 (br s, 6H), 1.83 (br s, 2H); λ_{max} (5% MeOH−CH_2Cl_2) 328 (ϵ = 750 cm^{-1} M^{-1}); HRMS (ES) *m*/*z* 361.0079 (calcd for $[C_{14}H_{15}O_2{}^{130}TeOH]^+$: 361.0083).

For **7** (95% yield): The ^{1}H NMR spectrum revealed a 55:45 mixture of two diastereomers at ambient temperature. At 50 °C, the signals for the two diastereomers sharpened (^{1}H NMR spectrum in Supporting Information). Major diastereomer: ^{1}H NMR (400 MHz, $CDCl_3$) δ 8.61 (d, 1H, *J* = 7.2 Hz), 7.2−7.8 (m's, 8H), 3.40 (q, 1H, *J* = 6.4 Hz), 2.25 (s, 6H), 1.42 (d, 3H, *J* = 6.4 Hz); minor diastereomer: δ 8.50 (d, 1H, *J* = 7.2 Hz), 7.2−7.8 (m's, 8H), 4.00 (q, 1H, *J* = 6.4 Hz), 2.16 (s, 6H), 1.22 (d, 3H, *J* = 6.4 Hz); λ_{max} (5% MeOH−CH_2Cl_2) 232 (sh) nm (ϵ = 720 cm^{-1} M^{-1}); HRMS (ES) *m*/*z* 372.0607 (calcd for $[C_{16}H_{19}N^{130}TeOH]^+$: 372.0607).

Reaction of PhSH with 5. A solution of PhSH (22 mg, 0.20 mmol) in 25 μL of CH_2Cl_2 was added to a solution of oxidized di-*n*-hexyl telluride **5** (34 mg, 0.10 mmol) in MeOH (975 μL). The resulting solution was stirred for 0.5 h and concentrated. The product mixture displayed a 1:1 mixture of PhSSPh and telluride **2** by ^{1}H NMR. The crude product was purified by flash chromatography on SiO_2 eluted with CH_2Cl_2 to give 20 mg (92%) of PhSSPh and 25 mg (83%) of **2** as a colorless oil.

For PhSSPh: mp 57−59 °C (lit.[6] mp 58−60 °C).

Reaction of PhSH with 6. A solution of PhSH (13 mg, 0.12 mmol) in 25 μL of CH_2Cl_2 was added to a solution of oxidized di-*p*-methoxyphenyl telluride **6** (0.022 g, 0.060 mmol) in MeOH (975 μL). The resulting solution was stirred for 0.5 h and concentrated. The crude product was purified by flash chromatography on SiO_2 eluted with CH_2Cl_2 to give 12 mg (93%) of PhSSPh and 15 mg (73%) of **3** as an off white solid, mp 47−49 °C.

Reaction of PhSH with 7. A solution of PhSH (22 mg, 0.20 mmol) in 25 μL of CH_2Cl_2 was added to a solution of oxidized (*S*)-(2-[1-(*N*,*N*-dimethylamino)ethyl]phenyl)phenyl telluride **7** (0.037 g, 0.10 mmol) in MeOH (975 μL). To this were added CH_2Cl_2 (25 μL) and thiophenol (20 μL, 22 mg, 0.2 mmol). The resulting solution was stirred for 0.5 h and concentrated. The crude product was purified by flash chromatography on SiO_2 eluted with CH_2Cl_2 to give 20 mg (92%) of PhSSPh and 26 mg (74%) of **4** as an off white solid, mp 71−73 °C; $[\alpha]^{20}_D$ = −4.99 (*c* = 1.02, $CHCl_3$).

Stopped-Flow Experiments. All stopped-flow experiments were performed on a SX18 Stopped-Flow spectrometer (Applied Photophysics, Leatherhead, UK). The sample-handling unit was fitted with two drive syringes that are mounted inside a thermostated-bath compartment, which allowed for variable-temperature experimentation. The optical detection cell was set up in the 2-mm path length. First- and second-order curve fitting and rate constants used a Marquardt algorithm[23] based on the routine Curfit.[24]

Preparation of Stock Solutions. A. Catalysis Experiments. Stock solutions of 2.0 × 10^{-3} M **2**−**4**, respectively, in CH_2Cl_2 and 5.0 × 10^{-2} M PhSH in CH_2Cl_2 were prepared. These were diluted with MeOH to give a 5% CH_2Cl_2/MeOH solution of 2.0 × 10^{-5} M telluride and 2.0 × 10^{-3} PhSH. A stock solution of 7.50 × 10^{-3} M H_2O_2 in MeOH was prepared. These two solutions were mixed in the stopped-flow spectrometer to give concentrations of 1.0 × 10^{-5} M telluride, 1.0 × 10^{-3} M PhSH, and 3.75 × 10^{-3} M H_2O_2, and the increase in absorbance at 305 nm was measured. The concentration of H_2O_2 in the stock solution was determined from the absorbance at 240 nm (ϵ = 43.6 cm^{-1} M^{-1}).[25]

B. Oxidation Experiments. The 2.06 × 10^{-3} M stock solutions of **2**−**4** in MeOH were diluted with MeOH to give 1.03 × 10^{-4} M solution of catalyst in MeOH. A stock solution of 2.06 × 10^{-1} M H_2O_2 in MeOH was prepared and diluted with MeOH to give 4.12 × 10^{-2}, 2.06 × 10^{-2}, and 1.03 × 10^{-2} M solutions of H_2O_2. The 1.03 × 10^{-4} M solution of telluride was mixed with each of the H_2O_2 solutions in the stopped-flow spectrometer to give the final concentrations indicated in Table S1 in the stopped-flow spectrometer. Kinetic traces were acquired at 276.8 ± 0.4 K at 352 nm for **2**, 330 nm for **3**, and 286 nm for **4**. For each concentration, 7−10 independent traces were averaged.

C. Thiophenol Exchange Elimination Experiments. Stock solutions of 2.06 × 10^{-3} M **5**−**7** were prepared. Dilution with MeOH gave 8.24 × 10^{-5} M solutions of **5** and **6** and 4.12 × 10^{-4} M solutions of **7**. A stock solution of 4.12 × 10^{-2} M PhSH in MeOH was prepared and was diluted with MeOH to give final concentrations of 1.65 × 10^{-3}, 8.24 × 10^{-4}, 4.12 × 10^{-4}, and 8.24 × 10^{-5} M solutions of PhSH for compounds **5** and **6** and 2.06 × 10^{-2}, 1.41 × 10^{-2}, 8.24 × 10^{-3}, 4.12 × 10^{-3}, 2.06 × 10^{-3}, 1.24 × 10^{-3}, 4.12 × 10^{-4}, and 8.24 × 10^{-5} M solutions of PhSH for compound **7**. The solution of oxidized telluride was mixed with the PhSH solutions to give the final concentrations indicated in Table S2 in the stopped-flow spectrometer. Kinetic traces were acquired at 276.8 ± 0.4 K at 300 nm for **2**, 300 nm for **3**, and 286 nm for **4**. For each concentration, 7−10 independent traces were averaged.

D. Reductive Elimination Experiments. Stock solutions of 2.06 × 10^{-3} M **5**−**7** were prepared. Dilution with MeOH gave 8.24 × 10^{-5}

(23) Marquardt, D. W. *J. Soc. Ind. Appl. Math.* **1963**, *11*, 431.
(24) Curfit is found in Bevington, P. R. *Data Reduction and Error Analysis for the Physical Sciences*; McGraw-Hill: New York, 1969.
(25) (a) Riley, J. C. M.; Berman, H. R. *Endocrinology* **1991**, *128*, 1749. (b) Zhao, G.; Bou-Abdallah, F.; Yang, X.; Arosio, P.; Chasteen, N. D. *Biochemistry* **2001**, *40*, 10832.

M solutions of **5** and **6** and 4.12×10^{-4} M solutions of **7**. A stock solution of 4.12×10^{-2} M PhSH in MeOH was prepared and was diluted with MeOH to give final concentrations of 3.30×10^{-2}, 2.88×10^{-2}, 2.48×10^{-2}, 2.06×10^{-2}, 1.65×10^{-2}, 1.24×10^{-2}, 8.24×10^{-3}, 3.30×10^{-3}, 2.48×10^{-3}, 1.65×10^{-3}, 8.24×10^{-4}, 4.12×10^{-4}, and 8.24×10^{-5} M solutions of PhSH. The solution of oxidized telluride was mixed with the PhSH solutions to give the final concentrations indicated in Table S3 in the stopped-flow spectrometer. Kinetic traces were acquired at 276.8 ± 0.4 K at 300 nm for **2**, 300 nm for **3**, and 286 nm for **4**. For each concentration, 7−10 independent traces were averaged.

E. Reactions with PhSOMe. A 0.08-M stock solution of benzenesulfenyl chloride (PhSCl) was prepared by the addition of 80 μL (135 mg, 1.0 mmol) of sulfuryl chloride to a solution of 0.24 g (1.1 mmol) of PhSSPh in 15 mL of 1,2-dichloroethane.[22] The reaction mixture was stirred for 5 min and was then diluted to 25 mL with 1,2-dichloroethane to give a final concentration of ~0.08 M in PhSCl. The solution of PhSCl was diluted with MeOH to 1.0×10^{-3} M, and the resulting solution was allowed to stand at ambient temperature for 15 min prior to mixing with 2.0×10^{-2} M PhSH in MeOH in the stopped-flow spectrometer at 276.8 ± 0.4 K. Kinetic traces were acquired at 305 nm to monitor the formation of PhSSPh, and the values of k_{obs} and ΔA s^{-1} represent the average of five independent runs.

Preparative Formation of PhSSPh from PhSOMe. Sulfuryl chloride (40 μL, 68 mg, 0.50 mmol) was added to a solution of 0.12 g (0.55 mmol) of PhSSPh in 5 mL of 1,2-dichloroethane. The resulting solution was stirred 5 min at ambient temperature and was then diluted with 20 mL of MeOH. Thiophenol (0.11 g, 1.0 mmol) in 5 mL of MeOH was added dropwise, and the resulting solution was stirred 2 h at ambient temperature. The reaction mixture was concentrated, and the residue was purified via chromatography on SiO_2 eluted with CH_2Cl_2 to give 0.20 g (92%) of PhSSPh, mp 57−59 °C, following recrystallization from 5% EtOAc/hexanes.

Acknowledgment. The authors thank the Office of Naval Research (N00014021-0836) and the National Science Foundation (CHE-0108521) for grants in support of this work.

Supporting Information Available: Figures S1−S3 showing electronic absorption spectra for **2**−**7**, Figures S4−S6 showing plots of k_{obs} as a function of H_2O_2 concentration for tellurides **2**−**4**, ^1H and ^{13}C NMR spectra and high-resolution electrospray mass spectrum for telluride **4**, electrospray ionization mass spectra for oxidized tellurides **5**−**7** in MeOH, ^1H NMR spectra for oxidized telluride **7** at 276 and 323 K, Table S1 for values of k_{obs} at various concentrations of H_2O_2 for the oxidation of **2**−**4**, Table S2 for values of k_{obs} at various concentrations of PhSH for reaction 1 in oxidized tellurides **5**−**7**, Table S3 for values of k_{obs} at various concentrations of PhSH for reaction 2 in oxidized tellurides **5**−**7**, general experimental conditions, and a discussion of the electrospray ionization mass spectra of **5**−**7** (PDF). This material is available free of charge via the Internet at http://pubs.acs.org.

JA029590M